Desulphurization of stainless steel by using $CaO-Al_2O_3$ based slags during secondary metallurgy

P. Yan[1], M. Guo[1], X. Guo[1], S. Huang[1], P.T. Jones[1], J. V. Dyck[1], J. Weytjens[2] and B. Blanpain[1]*

1) Department of Metallurgy and Materials Engineering, Katholieke Universiteit Leuven, Kasteelpark Arenberg 44 - Bus 2450, BE-3001 Leuven, Belgium

2) Aperam, Swinnenwijerweg 5 BE-3600 Genk, Belgium

Abstract: The desulphurization behavior of stainless steel by using lime-alumina based slag has been studied on a laboratory scale. The sulphur capacity of the slag was calculated with the aid of FactSage software. Consequently, the equilibrated sulphur distribution was then calculated. The effect of the experimental conditions, such as slag chemistry, temperature and oxygen level of the molten steel on the desulphurization behavior was investigated based on the experimental results and thermodynamic consideration. A kinetic model was developed to predict the evolution of sulphur content in molten steel as a function of time, and a good agreement between experimental data and modeling results was obtained. The sulphur removal rate in molten steel was found to be accelerated with increasing temperature and initial sulphur content in the steel. The desulphurisation capability of optimized lime-alumina based slag was found to be similar as that of lime-fluorspar based slag.

Key words: stainless steel; desulphurization; sulphur capacity; sulphur distribution; kinetic model

1. Introduction

The top slags used in the ladle metallurgy serve the important functions, such as, (i) to absorb impurities (e.g. sulphur and phosphorus) and inclusions from the liquid metal to form slag, (ii) to prevent the metal oxidation through air infiltration and (iii) to limit the heat losses during the secondary metallurgical process. In stainless steel production, after the scrap smelting in EAF and decarburization in AOD process, the AOD slag is removed and the top slag is added during the ladle treatment process. In the ladle treatment, a basic slag with high fluorine content (i.e. $CaO-SiO_2-CaF_2$) is commonly used due to its low melting temperature and high sulphur capacity. The final slag after the ladle treatment, however, disintegrates completely due to the β to γ phase transformation and is, therefore, not valorized at this moment. In order to solve the slag valorization issue, an option is to develop a fluorine free, non-disintegrating slag while at the same time not jeopardizing the quality of the steel products. In several countries such as Korea and Japan, CaF_2 has not been used anymore due to environmental related issues such as fluorine leaching from slag. The removal of CaF_2 from the system also provides several benefits (healthier environment on the work floor, lower refractory consumption in the casting ladles, avoiding any fluorine leaching issues etc.). Thus, alternatives for CaF_2 slag are being studied in EU countries.

The basic $CaO-Al_2O_3$ synthetic slag system is considered as a potential substitute for the $CaO-SiO_2-CaF_2$ slag. The slags from this system contain around 50-55 wt% CaO, 40-45 wt% Al_2O_3, ≤ 5 wt% SiO_2, ≤ 0.10 wt% C, and < 1 wt% FeO. Consequently, these slags have a low oxidation potential (low oxygen activity), a low melting temperature (which varies from 1350 to 1450 °C and reaches a minimum at around 42-48 wt% Al_2O_3) and a low viscosity (e.g. 0.16 to 0.36

Pa·s at temperatures between 1600 and 1700 °C). Therefore, from both the thermodynamic and kinetic point of view, this slag is an excellent refining agent, specifically for steel deoxidation and desulphurization. For example, experimental data for low carbon steels (1600 °C, [Al] = 0.01 wt%) have shown that lime saturated CaO-Al_2O_3-(SiO_2, MgO,) slags have a sulphur distribution ratios (L_S) > 10000[1].

The desulphurization, as one of the major considerations in the optimization of the secondary metallurgy slag, has been studied by several researchers. Xu *et al.* [2] found that the reaction rate of desulphurization through the permanent contact reaction increased remarkably with the increase of CaF_2 in the range of 0-10% in CaO based slag. Iwamasa *et al.*[3] confirmed that the existence of FeO in the CaO-SiO_2-MgO slag decreased sulphur distribution between the slag and steel and sulphur removal rate. Seshadri *et al.*[4] applied a kinetic model to investigate the desulphurization of molten pig iron by CaO based slag and indicated that the slag emulsion increased the sulphur removal rate. Andersson *et al.*[5] discussed the influence of the Al_2O_3/CaO ratio on sulphur capacity of CaO-Al_2O_3-SiO_2-MgO slag and concluded that the increase of the Al_2O_3/CaO ratio decreased the sulphur distribution between the slag and metal. Muhmood *et al.* [6] found that the low SiO_2 in CaO based slag resulted in a high sulphur diffusion coefficient and lead to a fast desulphurization rate. On the other hand, there are a number of literatures available for studies on the sulphur capacities in various slags[6-8]. However, they did not consider stainless steelmaking slags. So far, only a few papers on the slag control for desulphurization in the stainless steelmaking process has been available. The possibilities of the slag control with respect to desulphurization and slag valorization have not been fully explored for stainless steel refining.

In the present work, laboratory experiments by using CaO-Al_2O_3 based slags were performed to simulate secondary metallurgical process in stainless steel production. The sulphur capacity of the CaO-Al_2O_3 based slags was calculated with the aid of FactSage software. The effect of experimental conditions, such as slag chemistry, temperature and oxygen level of the molten steel on desulphurization was investigated based on the measured results and thermodynamic calculations. A kinetic model was developed to predict the evolution of sulphur in the molten steel as a function of time. Desulphurization capability of the CaO-Al_2O_3 based slags in the ladle treatment of stainless steelmaking was discussed in comparison with the CaO-CaF_2 based slags.

2. Experimental

2.1 Materials

To simulate the ladle treatment process of stainless steel production, an austenitic stainless steel (grade 302) ingot was collected after AOD process from a steel plant and it was employed in the laboratory experiments. Table 1 shows the chemical composition of the steel ingot. The compositions of the top slags used in the tests are listed in Table 2. The slag A, a mixture of lime (containing 94.5%CaO, 1.5%SiO_2 and 1.5%MgO, % represents mass percent hereinafter) and fluorspar (containing 90%CaF_2, 2.5%CaO and 5%SiO_2), is commonly used during ladle treatment in the stainless steel plant. The slag B and D are CaO-Al_2O_3 based synthetic slags (commercial products), which contain small amount of SiO_2, Fe_2O_3, MgO and TiO_2. The slag C is a mixture of the reagent grade oxides, i.e. CaO, Al_2O_3 and SiO_2.

Table 1. The chemical composition of austenitic stainless steel used in the tests (in wt%)

C	Mn	P	S	Si	Cr	Ni	Mo	Cu	Ti	Co	N	Al	B
0.03	1.2	0.03	0.0015	0.44	18.3	7.96	0.28	0.36	0.001	0.166	0.057	-	0.0006

Table 2. The chemical composition of top slag used in the tests (in wt%)

Slag type	CaO	Al_2O_3	Fe_2O_3	SiO_2	MgO	TiO_2	CaF_2
A	81.8	-	-	2.13	1.26	-	14.81
B	40.0	45.5	2.5	6.0	1.0	4.0	-
C	55.0	40.0	-	5.0	-	-	-
D	50.0	40.4	2.1	4.3	0.6	1.7	-

Apart from the steel and slags, ferroalloys, i.e. FeSi, FeMn and FeS and aluminum were also employed in the experiment. The composition of ferroalloys is given in Table 3.

Table 3. Chemical composition of the alloys employed in the laboratory experiment (in wt%)

Type of Ferroalloy	Si	Mn	S	Al	Fe
FeSi	75	-	-	2	23
FeS	-	-	38	-	62
FeMn	-	85	-	-	15
Al	-	-	-	100	-

2.2 Experimental procedure

The laboratory experiments were performed in a vacuum induction furnace (type VSG 30, 60 kW power supply and 4 kHz frequency). A schematic diagram of the experimental set-up is shown in Fig. 1. A loading chamber, a sampling device and a measurement tool were fitted on the furnace lid to allow slag addition, sampling, oxygen activity and temperature measurements. Fifteen kilograms of austenitic stainless steel was melted under Ar atmosphere in a magnesia crucible with inner diameter of 150 mm, outer diameter of 176 mm and the height of 275 mm, and with compositions of 88%MgO, 3.5%Al_2O_3, 3.8%SiO_2 and 3.8%CaO. The temperature of molten steel was controlled at 1600 to 1650 ℃, followed by the addition of 8 g FeS alloy and 12 g FeMn alloy. Thereafter, the oxygen activity and temperature of the molten steel were measured with Celox type B (provided by Heraeus Electro-Nite) and thermocouple type B, respectively. Subsequently, a steel sample in conical shape (the upper diameter is 20 mm, lower diameter is 10 mm and the height is from 16 to 25 mm) was taken by dipping the spoon sampler into the liquid bath and rapidly withdrawing it, followed by quenching. Then, a certain amount of slag together with 50 g FeSi alloy were added to the molten steel through the loading chamber, meanwhile 3 g Al was added to molten steel in Test No. 3, 5, 6 and 7, and the bottom Ar stirring was introduced in Test No. 6. After the first addition of the slag, the steel sample was taken at desired time, then immediately followed by the second slag addition and another steel sampling at desired time. The same procedure was followed for the third and fourth slag addition and sampling. The detailed experimental conditions are listed in Table 4. At the end of the test, the temperature and oxygen activity of the molten steel were measured, then the melt was poured into a mould. The slag sample was collected after the cooling down of the mould.

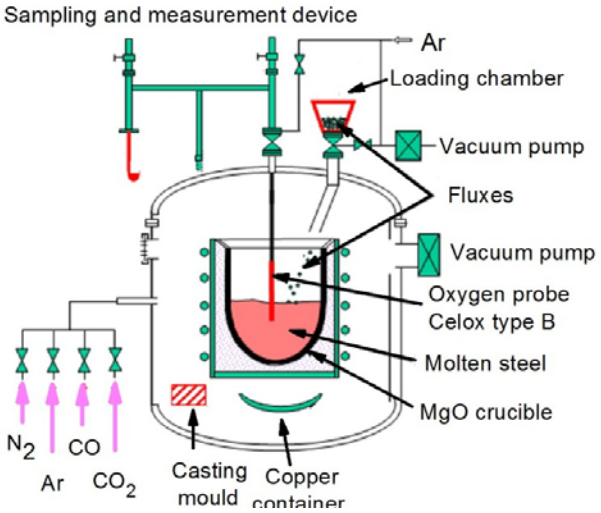

Fig. 1. Schematic diagram of the experimental set-up

Table 4. Experimental conditions and procedures for each test

Test No.	Slag type	Slag addition (g)				FeSi (g)	Al (g)	Argon Stirring (L/min)
		1st	2nd	3rd	4th			
1	A	150	225	0	0	50	0	0
2	B	225	0	150	75	50	0	0
3	C	150	150	150	150	50	3	0
4	C	150	150	150	150	50	0	0
5	C	150	150	150	150	50	3	0
6	C	150	150	150	150	50	3	0.9
7	D	150	150	150	150	50	3	0

2.3 Sample analysis

The steel samples obtained during the tests were used for sulphur content measurement by LECO combustion analysis (type CS-444, based on infrared absorption). The accuracy of sulphur analysis for CS-444 is ±4 ppm. Each steel sample was cut into small pieces (0.5-1.0 g) and cleaned with ultrasonic bath. At least two pieces of steel samples were analyzed and the average sulphur amount was used as the total sulphur content in the steel sample. The slag composition was analyzed with X-ray fluorescence spectrometer (XRF, Philips PW 2400). The slag was collected after the mould cooled down and crushed into small fragments (< 4 mm) with Jaw crusher, followed by a centrifugal grinding mill to reduce the particle size to 80 μm. The Sieves with a size of 0.5 mm and 0.08 mm were used during the milling. Then the milled slag sample was collected in a container and uniformly mixed. Five grams of milled slag sample was gathered and analyzed with XRF spectrometer. The total sulphur amount of the slag was also analyzed with LECO equipment.

3. Results and discussion

3.1 Desulphurization results

In all the tests, sulphur content was measured for steel samples and slags. The oxygen activity and temperature of the molten steel were measured before the first slag addition and at the end of test. The experimental results for the steel

samples are summarized in Table 5. The slag composition was measured after the test and listed in Table 6, where [S] and (S) represent the total sulphur content in steel and slag, respectively, $a_{[O]}$ represents oxygen activity in molten steel. The evolution of [S] in molten steel as a function of time is illustrated in Fig. 2. The sulphur distribution between the slag and steel, i.e. L_S=(S)/[S], and the average [S] removal rate are shown in Fig. 3.

Table 5. The LECO analysis results of the steel samples, and the $a_{[O]}$ and temperature of the molten steel

Test No.	Slag type	Sample No.	Time after 1st slag addition (min)	[S] (ppm)	Temp. (°C)	$a_{[O]}$ (ppm)
		T1-0	0	105	1599	21
		T1-1	24	35	-	-
1	A	T1-2	42	14	-	-
		T1-3	51	14	-	-
		T1-4	60	15	1607	17.1
		T2-0	0	157	1601	27
		T2-1	14	148	-	-
2	B	T2-2	24	136	-	-
		T2-3	40	117	-	-
		T2-4	60	110	1626	20.7
		T3-0	0	223	1673	47
		T3-1	8	175	-	-
3	C	T3-2	20	133	-	-
		T3-3	35	101	-	-
		T3-4	57	79	1612	14.8
		T4-0	0	142	1652	39
		T4-1	10	123	-	-
4	C	T4-2	20	97	-	-
		T4-3	35	83	-	-
		T4-4	45	60	1590	17.0
		T5-0	0	138	1597	18
		T5-1	10	100	-	-
5	C	T5-2	21	60	-	-
		T5-3	34	43	-	-
		T5-4	49	29	1659	23.8
		T6-0	0	-	1597	22
		T6-1	12	119	-	-
6	C	T6-2	27	105	-	-
		T6-3	42	84	-	-
		T6-4	57	62	1635	22.5
		T7-0	0	232	1601	25
		T7-1	10	230	-	-
7	D	T7-2	20	85	-	-
		T7-3	35	59	-	-
		T7-4	50	37	1679	19.0

Table 6. The chemical composition of slag and the sulphur distribution between the slag and steel after the tests

Test No.	wt %							(S) (ppm)	L_S
	CaO	SiO_2	MgO	Al_2O_3	Cr_2O_3	Fe_2O_3	MnO		
T1	58.3	19.7	9.42	9.17	1.03	1.15	0.70	1155	77
T2	43.7	5.02	2.82	44.8	0.88	1.56	0.44	1650	15
T3	42.6	8.87	5.50	43.0	-	-	-	3400	43
T4	36.0	18.7	7.65	31.3	5.26	-	1.02	1400	23
T5	51.6	8.76	4.06	36.0	-	-	-	1200	41
T6	44.2	9.65	4.50	41.3	-	-	-	2000	32
T7	50.9	6.62	3.80	38.6	-	-	-	2900	80

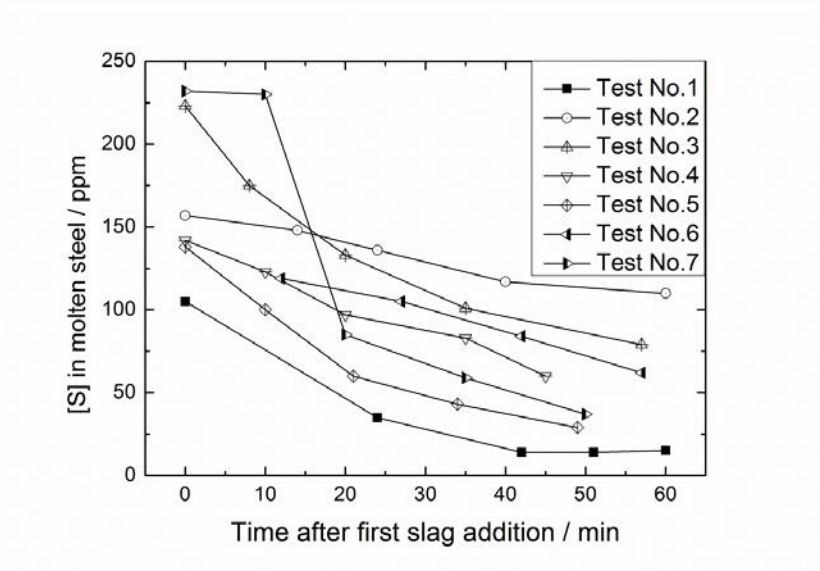

Fig. 2. The evolution of [S] in molten steel as a function of time after first slag addition

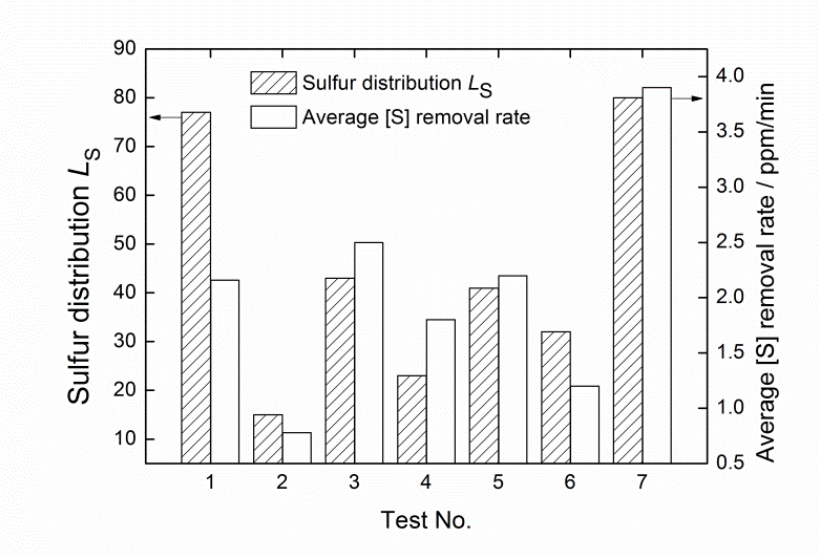

Fig. 3. The sulphur distribution L_S between the slag and steel and the average [S] removal rate in each test

According to the preceding summary of the experimental results (shown in Tables 5 and 6 and in Figs. 2 and 3), qualitative understandings can be described as followings with respect to the desulphurization:

(1) The sulphur is continuously transferred from the molten steel to the slag with treatment time. All slags show desulphurization capability. For most of the tests (except Test No.2) there is a tendency that after the slag addition, the [S] is rapidly removed in early stage, and then dropped slowly or kept constant at a low level until the completion of the test (Fig. 2).

(2) Top slag type (chemical composition) significantly affects the sulphur removal efficiency. As shown in Figs. 2 and 3, under similar test conditions i.e. initial sulphur content, oxygen content, treatment temperature and stirring circumstance, type D slag (Test No. 7) exhibits a higher desulphurization capability than type C slag (Test No.3). Tests (No. 4 & 5) with the type C slag show better desulphurization results than the Test No. 2 with type B slag. According to the final sulphur distribution between the slag and steel (Fig. 3), a comparable desulphurization effect is achieved with

the type D (Test No. 7) and type A (Test No. 1) slags. However, the average [S] removal rate is lower for the type A slag, which is due to the lowest initial sulphur content of the steel in the case of Test No. 1.

(3) Besides the influence of the top slag chemistry, the desulphurization behavior is affected with initial sulphur content and oxygen level of the steel. As expected, sulphur is removed easily from the steel with higher initial sulphur content as can be seen in Figs.2 & 3 for Test No. 3 (type C slag and 223 ppm initial [S]) and Test No.5 (type C slag and 138 ppm initial [S]). On the other hand, for Test No. 4 and 5, different desulphurization effect for similar initial conditions (type C slag and initial sulphur content) suggests the influence of the oxygen level. A better desulphurization is observed in Test No. 5 with aluminum deoxidation than in Test No. 4 without it.

(4) The influence of kinetic condition on the desulphurization is investigated in Test No. 6 with bottom Ar blowing. As can be seen in Figs 2 and 3, a poor desulphurization is observed in Test No. 6 as compared to the Test No. 5, which has similar test conditions (i.e. slag type C, 3 grams aluminum deoxidation, around 140 ppm initial [S] and temperature ranging from 1600 to1650 °C) with the exception of bottom Ar blowing in Test No. 6. According to the visual observation during the test, bottom Ar blowing pushes the top slag onto the crucible wall, which leads to a large open eye in the slag/metal bath, reducing slag/metal contact area and therefore weakening the desulphurization kinetics. This inversely confirms the kinetic effect on the desulphurization reaction. Further work is necessary to improve the present experimental set-up to precisely control the reaction kinetics.

3.2 Thermodynamic consideration on the desulphurization

Sulphur capacity C_S, a function of slag composition and temperature, is defined as a measurement of the sulphur absorption ability of metallurgical slag by Fincham and Richardson[7],

$$C_S = \exp\left(-\frac{\Delta G^0}{RT}\right)\cdot\left(\frac{a_{(O)}}{f_{(S)}}\right) \tag{1}$$

where $a_{(O)}$ is the activity of oxide ions in the slag; $f_{(S)}$ is the activity coefficient of sulfide ions in the slag; R is the gas constant, 8.314 J/(mol·K); T is the temperature in K; ΔG^o is the Gibbs energy of the following reaction, J/mol:

$$\frac{1}{2}S_2(g) + \left(O^{2-}\right) = (S^{2-}) + \frac{1}{2}O_2(g) \qquad \Delta G^o = 118535 - 58.8157T \tag{2}$$

by combining the definition of sulphur capacity (i.e. Eq. (1)) and the reaction (2), the sulphur capacity of the slag can be expressed as follow:

$$C_S = (\%S)\cdot\left(\frac{P_{O_2}}{P_{S_2}}\right)^{\frac{1}{2}} \tag{3}$$

where (%S) is the weight percentage of sulphur content in the slag; P_{O_2} and P_{S_2} are partial pressures of O_2 and S_2 gas in the system, Pa.

In general, the sulphur capacity can be measured through the classical gas ($CO+CO_2+SO_2+Ar$)/liquid slag equilibrium experiment. There are also several mathematical models[8-10] developed for the sulphur capacity calculation. In order to better understand the desulphurization results obtained in the tests, the sulphur capacities of the slag systems,

which were employed in the present tests, is evaluated with the aid of FactSage software. In the calculation, the thermodynamic equilibrium between the slag and a gas mixture (CO: CO_2: SO_2: Ar = 5: 4: 1: 10) at specific temperature is calculated with the Equilibrium module in the FactSage. On substitution of the equilibrated mole amount of O_2 (g) and S_2 (g), as well as the equilibrated sulphur content in slag into Eq. (3), the sulphur capacity can be estimated. It should be noted that the initial chemistry of the gas mixture would not influence the final result of the sulphur capacity in the calculation. The database of FACT and FToxid were used in the calculation. The calculated results at 1873 K for CAS-14.4%CaF_2 (CAS represents CaO-Al_2O_3-SiO_2), CAS-2.5%Fe_2O_3-1%MgO-4%TiO_2, CAS and CAS-2.1%Fe_2O_3-0.6%MgO-1.7%TiO_2 slag systems, which respectively correspond to slag A, B, C and D, are shown in Fig. 4. The solid points in Figs. 4a, 4b, 4c and 4d represent the initial composition of the slag A, B, C and D, respectively. The open symbols represent the final composition of the slags after the tests. It should be mentioned that these data points are not the exact composition of the slag, because the minor compounds are neglected to integrate the slag into the figure with three principle components, i.e. CaO, SiO_2 and Al_2O_3. The calculated sulphur capacity values for the initial slag and the final slag from Test No. 1 to 7 are listed in Table 7. The exact composition and the measured temperature are used in these calculations.

It can be seen from Fig. 4 that the sulphur capacity increases with the increase of %CaO and decreases with the increase of %SiO_2 and %Al_2O_3 in CA based slag. The melting temperature of CA based slag is high in CaO rich region. Based on the results of Fig. 4 and Table 7, it can be concluded that (1) slag B has the lowest sulphur capacity while slag A shows the highest one, which is because of the slag chemistry, mainly due to difference in the CaO content in these two slags; (2) under same temperature, larger liquid area are observed with CAS-2.5%Fe_2O_3-1%MgO-4%TiO_2 (Fig. 4b) and CAS-2.1%Fe_2O_3-0.6%MgO-1.7%TiO_2 (Fig. 4d) slag systems as compared to the CAS-14.4%CaF_2 (Fig. 4a) and CAS (Fig. 4c) slag systems. This indicates that minor additions of Fe_2O_3, MgO and TiO_2 to the slag lowers the melting temperature of the slags, and would facilitate the desulphurization kinetics; (3) slag composition slightly changed after the treatment and remained on the lime saturated liquidus for the pre-melted synthetic slags (Figs. 4b and 4d), while it moved toward to the lower sulphur capacity direction for the tests with the slags (Figs. 4a and 4c) consisting of the mixtures of oxides and calcium fluoride. The later implies that the desulphurization capability of the mixture slags decreases as reaction proceeds. This is not the case for the pre-melted synthetic slags, suggesting advantages of chemical and physical homogenization of the slags for the desulphurization; (4) the iso-log C_S curves are parallel to the lime saturated liquidus and the C_S value increases with the curves being close to the lime saturated liquidus. This indicates a necessary optimization of the slags for the desulphurization with respect to its thermodynamic and kinetic properties, i.e. sulphur capacity and viscosity of the slags. If the kinetics allows, CaO saturated slags are recommended for the desulphurization refining practice.

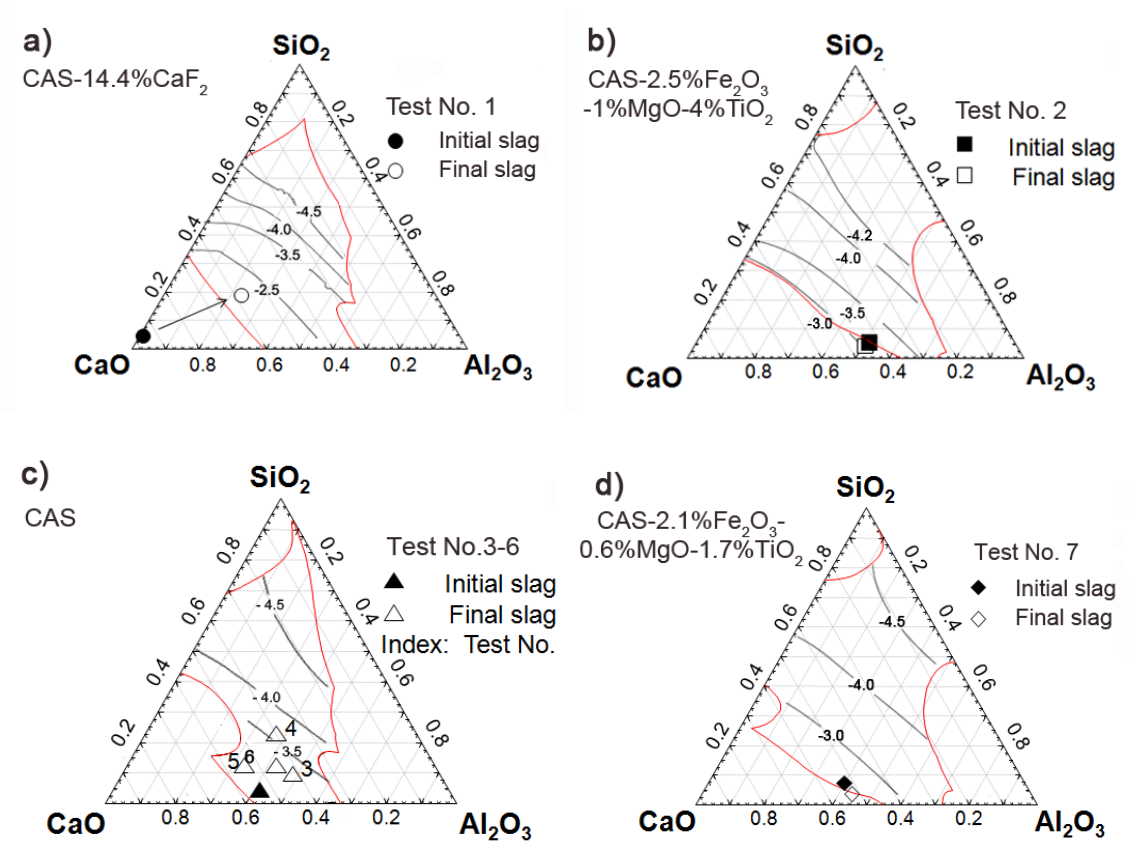

Fig. 4. Iso-log C_S contours of the slags at 1600 ℃, a) CAS-14.4%CaF_2, b) CAS-2.5%Fe_2O_3-1%MgO-4%TiO_2, c) CAS and d) CAS-2.1%Fe_2O_3-0.6%MgO-1.7%TiO_2 slag systems

Table 7. The calculated sulphur capacity for the initial slag and the final slag through Test No. 1 to 7

C_S	T1	T2	T3	T4	T5	T6	T7
Initial slag	2.2×10^{-1}	1.1×10^{-3}	4.9×10^{-3}	4.7×10^{-3}	5.7×10^{-3}	5.3×10^{-3}	4.4×10^{-3}
Final slag	3.9×10^{-2}	3.1×10^{-3}	2.3×10^{-3}	1.0×10^{-3}	8.2×10^{-3}	2.9×10^{-3}	8.8×10^{-3}

The measured sulphur distribution L_S are plotted against the calculated sulphur capacity C_S in logarithmic scale in Fig. 5. It can be seen from Fig. 5 that the data points follow approximately the line with the slope of 1. This indicates that the sulphur distribution is mainly determined by the sulphur capacity of slag. In other word, with similar desulphurization conditions, the slag with high sulphur capacity has a strong sulphur absorption ability and leads to a larger sulphur distribution.

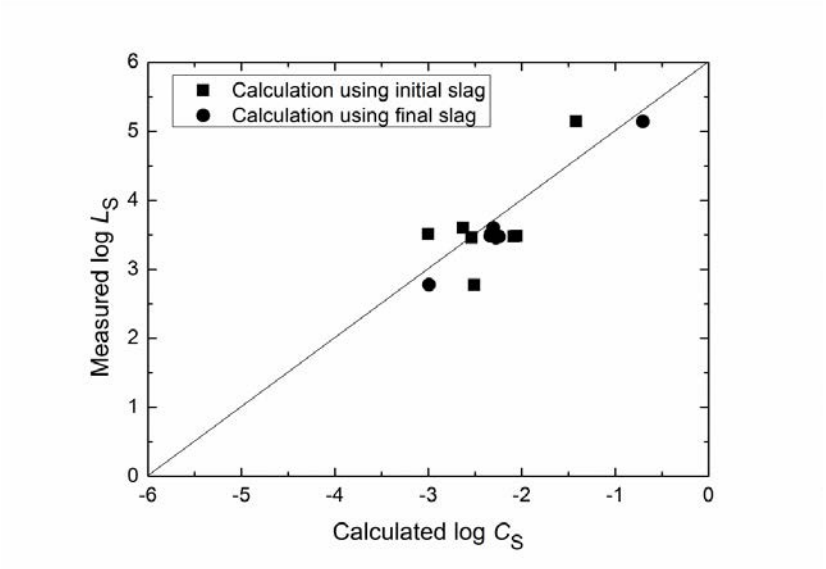

Fig. 5. Relation between the measured sulphur distribution L_S and the calculated sulphur capacity C_S in logarithmic scale

In steelmaking practice, the sulphur distribution between slag and steel, i.e. L_S, is used to indicate the desulphurization effect of slag. In order to investigate the influence of sulphur capacity and desulphurization conditions on the sulphur distribution, the gas-slag equilibrium (reaction 2) and slag-metal equilibrium (reaction 4) are combined into a new gas-metal equilibrium as given by reaction (5)[11]. Consequently, the relation between the sulphur capacity and the equilibrated sulphur distribution can be expressed as Eq. (6):

$$[\mathrm{S}] + (\mathrm{O}^{2-})_{\mathrm{slag}} = [\mathrm{O}] + (\mathrm{S}^{2-})_{\mathrm{slag}} \tag{4}$$

$$[\mathrm{S}] + \frac{1}{2}\mathrm{O}_2(\mathrm{g}) = [\mathrm{O}] + \frac{1}{2}\mathrm{S}_2(\mathrm{g}) \tag{5}$$

$$\log L_S = \log \mathrm{K}_5 + \log C_S + \log f_{[\mathrm{S}]} - \log a_{[\mathrm{O}]} \tag{6}$$

where K_5 is the equilibrium constant of the Eq. (5), and $\log \mathrm{K}_5 = -\frac{935}{T} + 1.375$; $f_{[\mathrm{S}]}$ is the activity coefficient of sulphur in molten steel. Furthermore, the activity coefficient of sulphur $f_{[\mathrm{S}]}$ in Eq. (6) can be calculated by using Wagner's equation[12],

$$\log f_{[j]} = \sum (e_j^i [\%i] + r_j^i [\%i]^2) \tag{7}$$

where *i* represents the dissolved element in molten steel; e_j^i and r_j^i are the interaction parameter of *i* for *j* element (see Table 8).

It can be seen from Eq. (6) that the equilibrated $\log L_S$ and $\log C_S$ has the linear relation, which was verified in the present work as shown in Fig. 5. In addition to the sulphur capacity of slag, which is mainly relevant with slag chemistry, other parameters, such as steel chemistry, operation temperature and kinetic conditions could also affect the sulphur distribution of the desulphurization practice. The composition of the steel has complex influence on sulphur

distribution due to its effect on the sulphur and oxygen activity in molten steel.

Table 8. Interaction parameters used in the calculation

i	e_i^{O}	e_i^{Si}	e_i^{Cr}	r_i^{Cr}	e_i^{Ni}	r_i^{Ni}	e_i^{Mn}	e_i^{S}	e_i^{C}	reference
Si	-0.119	0.103	-0.021	4.3×10^{-4}	-0.009	2×10^{-4}	0.033	0.056	0.18	[13-15]
S	0.27	0.065	0.01	0	0	0	-0.025	-0.028	0.113	[15, 16]

Substituting interaction parameters (shown in Table 8), steel composition, oxygen activity of the molten steel, operation temperature, and calculated sulphur capacity (shown in Table 7), respectively into Eq. (6) and (7), the sulphur distribution (L_S) can be calculated. Fig. 6 shows comparison of the measured and the calculated sulphur distribution value, which in the upper diagram of Fig. 6 is obtained by using the chemistry of the initial slags and in the lower diagram by that of the final slags. The results in Fig. 6 demonstrated that (1) relation between the calculated and measured sulphur distribution follows approximately a straight line, which is parallel to the one by one relationship, i.e. the dashed lines in Fig. 6, suggesting an reliable assessment for both calculated and measured L_S data; (2) the calculation is more reasonable when using the chemistry of the final slags; (3) the calculated log L_S (thermodynamic equilibrium) value is around one time larger than the measured value. This means that the slag/molten steel interaction was far from equilibrium with respect to the desulphurization reaction in the present tests. Therefore, desulphurization capabilities of the top slags have not been fully utilized in the present pilot ladle treatment. If the kinetics allows, the desulphurization effect can certainly be improved by using the current top slags. In the following section, the desulphurization kinetics is discussed with respect to the experimental conditions.

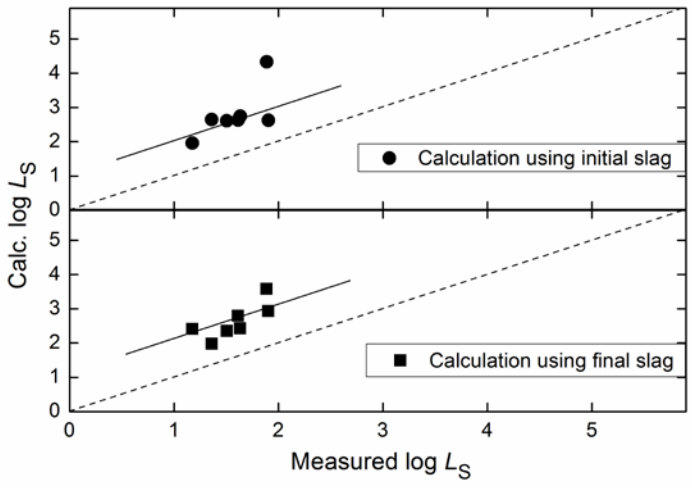

Fig. 6. Comparison between the measured and calculated sulphur distribution L_S in logarithmic scale

3.3 Desulphurization kinetics

Mathematical model

To better understand the desulphurization behavior in the pilot experiments, a kinetic model is developed to predict sulphur evolution in the molten steel during the tests. The model is based on the two film theory that the dissolved sulphur is removed by permanent contact reaction at the interface between molten steel and slag. A schematic

representation of the desulphurization kinetics is illustrated in Fig. 7, where $C_{[i]}$, $C_{(i)}$, $C^{i}_{[i]}$ and $C^{i}_{(i)}$, respectively represent the concentration of species *i* in molten steel, in slag, at the interface towards molten steel and at the interface towards slag. According to Fig. 7, the desulphurization process can be divided into the following kinetic steps:

(1) [S] is transferred from molten steel towards the slag, meanwhile the (O) is transferred from the slag towards the steel bath.

(2) [S] and (O) are exchanged at the slag/steel interface through the desulphurization reaction, i.e. Eq. (4).

(3) [O] and (S) are transferred from the slag/steel interface towards steel and slag phase, respectively.

To simplify the mathematical model and calculation, the following assumptions were made: (a) there is no species (i.e. reactants and products) accumulated at the interface; (b) slag is uniformly covered on the surface of molten steel; (c) the dissolved elements, such as sulphur and oxygen, are homogeneously distributed in the steel phase at the beginning of the experiments; (d) chemical reaction at the interface is fast enough for not being the rate-limiting step of the desulphurization; (e) chemical ractions at the interface reached equilibrium.

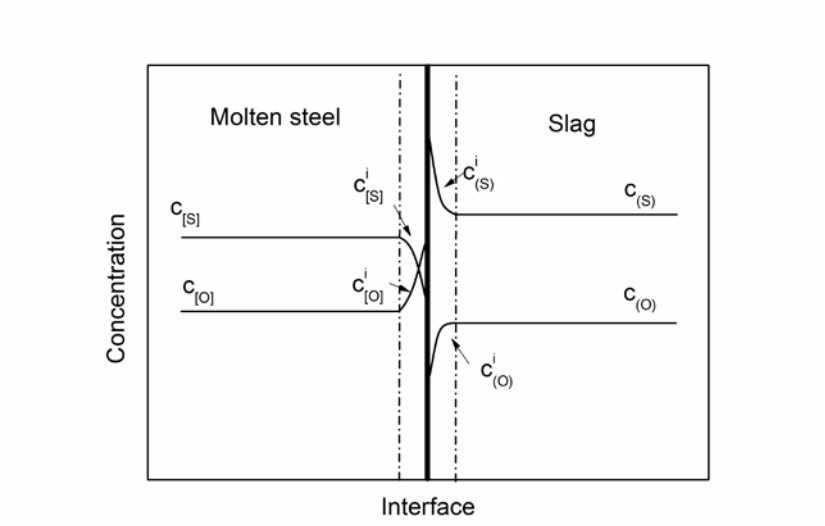

Fig. 7. A schematic representative of the desulphurization kinetics

In general, possible rate controlling steps of the desulphurization are considered to be the mass transport aspects, such as transfer of [S] from molten steel towards the reaction interface, (S) from the interface towards bulk slag phase, (O) from slag towards the interface and [O] from the interface towards molten steel. According to the previous studies[2, 4, 17], transfer of (S) from the interface to bulk slag is substantiated to be the rate controlling step of the desulphurization reaction. Therefore, desulphurization rate can be expressed in terms of the flux of (S) in slag phase, which is written as Eq. (8):

$$J = k_m (C_{[S]} - C^{i}_{[S]}) = k_s (C^{i}_{(S)} - C_{(S)}) \quad (8)$$

where *J* is the sulphur flux in slag phase, mol/(m^2·s); k_m and k_s are the mass transfer coefficient of sulphur, respectively, in steel and slag phase at the permanent contact reaction zone, m/s. Thus, sulphur removal rate in molten steel can be calculated as follow:

$$-\frac{d[\mathrm{S}]}{dt}=\frac{W_s\cdot A\cdot k_s}{W_m\cdot V_s}\left\{(S)_i^t-(\mathrm{S})^t\right\} \tag{9}$$

in which

$$(\mathrm{S})_i^t=L_S[\mathrm{S}]^t \tag{10}$$

where A is contact area between the slag and steel, m^2; V_s is the volume of slag at time t, m^3; W_m and W_s are the weight of molten steel and slag at time t, kg, respectively; $(\mathrm{S})_i^t$, $(\mathrm{S})^t$ and $[\mathrm{S}]^t$ are the sulphur content at the interface, in slag, and in steel at time t, ppm, respectively. Thanking the mass balance of sulphur between the steel and the slag into account, (S) in slag at time t can be expressed by Eq. (11),

$$(\mathrm{S})^t=\frac{W_m([\mathrm{S}]^o-[\mathrm{S}]^t)}{W_s} \tag{11}$$

where $[\mathrm{S}]^o$ is the sulphur content in the steel at time = 0 s, ppm. Combining the Eqs. (9) to (11), following equation is derived:

$$\ln\left\{(L_S+\frac{W_m}{W_s})[\mathrm{S}]^t-\frac{W_m}{W_s}[\mathrm{S}]^\circ\right\}=-\frac{A\cdot\rho_s\cdot k_s}{W_m}(L_S+\frac{W_m}{W_s})t+\ln\left\{L_S\cdot[\mathrm{S}]^\circ\right\} \tag{12}$$

where ρ_s is the density of slag at experiment temperature, kg/cm^3. Furthermore, the mass transfer coefficient k_s can be calculated by using the empirical equation (13) [4, 17, 18]:

$$k_s=\beta\sqrt{D_S\frac{Q}{A}} \tag{13}$$

$$Q=\frac{Q^oTP_a}{273P} \tag{14}$$

where β is empirical coefficient, 1 $m^{-1/2}$; D_S is the sulphur diffusivity in the slag, m^2/s; Q^o is total gas flow rate, m^3/s; P_a is the standard atmospheric pressure and P is the gas pressure in the furnace, Pa.

The diffusivity of sulphur in CAS based slag is estimated by using the model developed by Muhmood *et al.* [6],

$$\log(D_S)=-\frac{1166.5}{T}-8.7063 \tag{15}$$

The density of CAS slag ρ_s is estimated by using the model developed by Persson[19],

$$\rho_s=\frac{\sum_i X_iM_i}{\sum_i X_iV_{mi}(1+\frac{\lambda H_m}{R\mathrm{T}})} \tag{16}$$

where V_{mi} is molar volume for the pure substance of i, cm^3/mol; ρ_i is the density of pure substance of i at experimental temperature, g/cm^3; H_m is the relative integral molar enthalpy, J/mol; X_i and M_i are the mole fraction and molecular mass of i component, respectively and λ is a constant, 0.06.

The V_{mi} can be calculated by empirical equation developed by Muhmood[20],

$$V_{mi}=\frac{M_i}{\rho_i} \tag{17}$$

$$\rho_{Al_2O_3} = 3.04 - 1.15\times10^{-3}(\mathrm{T}-2303) \quad (18)$$

$$\rho_{SiO_2} = 3.0451 - 4\times10^{-4}\,\mathrm{T} \quad (19)$$

$$\rho_{CaO} = 3.4151 - 2\times10^{-4}\,\mathrm{T} \quad (20)$$

Substituting experimental parameters estimated through Eqs. (13) to (20) into Eq. (12), evolution of sulphur content in the molten steel during the ladle refining can be calculated.

Calculated results

The experimental parameters used in the calculations are summarized in Table 9. The prediction of [S] evolution as a function of time is calculated for Test No. 3 to 6. In the calculation, the value of 4.7×10^{-10} m^2/s is used for sulphur diffusivity calculation[6]. The gas flow rate of 0.5 L/min, the furnace pressure of 5 Bar and the temperature at end of the test are used for the calculation of mass transfer coefficient of sulphur in the slag phase (k_s). Since the slag covered only around 1/4 molten steel surface (as shown in Fig. 8) during the test, the steel/slag contact area was considered to be 1/4 of the cross section area of the crucible in the calculation. For comparison, both the experimental and calculated results are plotted in Fig. 9.

Table 9. The experimental parameters used in the calculations

Test No.	L_S	T (°C)	ρ (g/cm^3)	D_S (m^2/s)	A (m^2)	k (m/s)	[S]° (ppm)
3	445	1612	2.79	4.7×10^{-10}	4.4×10^{-3}	1.15×10^{-6}	223
4	430	1590	2.80	4.7×10^{-10}	4.4×10^{-3}	1.15×10^{-6}	142
5	407	1659	2.78	4.9×10^{-10}	4.4×10^{-3}	1.15×10^{-6}	138
6	423	1635	2.79	4.8×10^{-10}	4.4×10^{-3}	1.15×10^{-6}	119

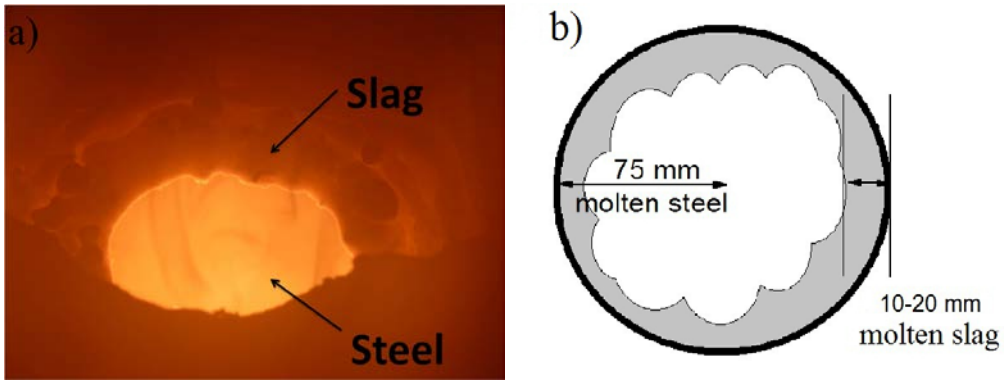

Fig. 8. The situation of the sleel/slag contact during the tests: (a) picture of the slag and steel in the crucible during experiment; (b) schematic diagram of the steel/slag contact

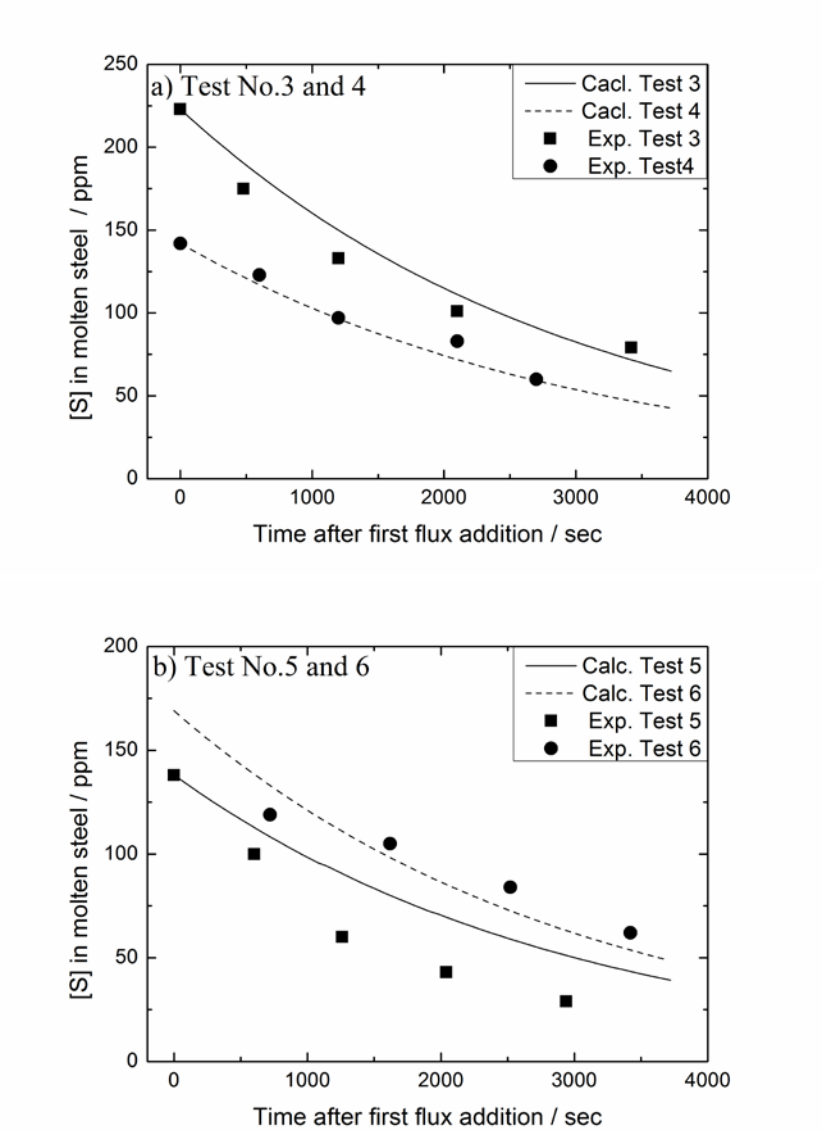

Fig .9. Comparison of the experimental and calculated results for sulphur evolution during the desulphurization refining: (a) results of the Test No.3 and 4; (b) results of the Test No. 5 and 6

Figure 9 shows that except for Test No.5, the calculated sulphur evolutions are in a good agreement with experimental data. This suggests that (1) the assumption of the present calculation is reasonable, in which desulphurization occurs through the slag/steel permanent contact reaction and the mass transfer of (S) in slag phase is considered to be the rate controlling step of the desulphurization reaction; (2) desulphurization is not enhanced through the bottom Ar gas stirring (Fig. 9b), comparison of Test No.5 and 6) in the experiment. This can be understood with the visual observation that bottom Ar blowing pushed the top slag onto the crucible wall, reducing slag/metal contact area and therefore, weakening the desulphurization kinetics; (3) desulphurization rate decreases with the decreasing of the sulphur content in the steel, implying the difficulty of the ultra-low sulphur steel refining. In the case of Test No. 5 (Fig. 9b), the desulphurization rate is underestimated by the calculation. The reason for this underestimation is not clear and it is probably due to a low sulphur analysis in the slag phase. Further work is necessary to improve the present mathematical model for its industrial application on the ladle treatment practice.

4. Conclusion

The desulphurization of austenitic stainless steel by using the lime-alumina based slags has been studied. The sulphur capacity was calculated based on the experimental data with the aid of FactSage software. The effect of sulphur capacity and experimental conditions on the desulphurization was investigated based on the thermodynamic consideration. A desulphurization kinetic model was developed for the prediction of sulphur evolution in the steel during the ladle treatment. The main results can be summarized as follow:

(1) The iso-sulphur capacity curves at 1600 °C were calculated with respect to the $CaO\text{-}Al_2O_3$ based slag and $CaO\text{-}CaF_2$ based systems. The iso-log C_S curves are parallel to the lime saturated liquidus and the C_S value increases with the curves being close to the lime saturated liquidus. If the kinetics allows, CaO saturated slags are recommended for the desulphurization refining practice.

(2) Experimental results showed that slag and steel chemistry, temperature, bottom Ar blowing had complex influences on the desulphurization, which is, however, mainly determined by the sulphur capacity of the slags. A comparable desulphurization effect was obtained with an optimized lime-alumina based slag as with the lime-fluorspar based slags.

(3) A kinetic model based on the slag/steel permanent contact reaction was established for the desulphurization. The calculated sulphur evolutions in the steel during the pilot tests were in a good agreement with experimental data, suggesting a promising industrial application of the model on the ladle treatment practice.

References

[1] Hino, M. and S. Ban-ya, Equilibria of Sulphur and Oxygen Between $CaO\text{-}Al_2O_3$ Based Slags and Liquid Iron. *Ultra High Purity Base Metal*, ed. K. Abiko, K. Hirokawa, and S. Takaki. 1995, Sendai, Japan: The Japan Institute of Metals.

[2] Chushao, X. and T. Xin, Kinetics of desulfurization of hot metal by $CaO\text{-}CaF_2$ based fluxes. *ISIJ international*, 1992. 32(10): p. 1081-1083.

[3] Iwamasa, P. and R. Fruehan, Effect of FeO in the slag and silicon in the metal on the desulfurization of hot metal. *Metallurgical and Materials Transactions B*, 1997. 28(1): p. 47-57.

[4] Seshadri, V. and C. da Silva, A kinetic model applied to the molten pig iron desulfurization by injection of lime-based powders. *ISIJ International*, 1997. 37(1): p. 21-30.

[5] M.A.T. Andersson, P.G.J., and M.Hallberg, Optimisation of ladle slag composition by application of sulphide capacity model. *Ironmaking & Steelmaking*, 2000. 27: p. 286-293.

[6] Muhmood, L., et al., Evaluating the Diffusion Coefficient of Sulfur in Low-Silica $CaO\text{-}SiO_2\text{-}Al_2O_3$ Slag. *Metallurgical and Materials Transactions B*. 42(2): p. 274-280.

[7] Fincham, C. and F. Richardson, The behaviour of sulphur in silicate and aluminate melts. *Proceedings of the Royal Society of London. Series A.* Mathematical and Physical Sciences, 1954. 223(1152): p. 40.

[8] Sosinsky, D.J. and I. Sommerville, The composition and temperature dependence of the sulfide capacity of metallurgical slags. *Metallurgical and Materials Transactions B*, 1986. 17(2): p. 331-337.

[9] Nzotta, M., D. Sichen, and S. Seetharaman, A study of the sulfide capacities of iron-oxide containing slags. *Metallurgical and Materials Transactions B*, 1999. 30(5): p. 909-920.

[10] Young, R., et al., Use of optical basicity concept for determining phosphorus and sulphur slag- metal partitions. *Ironmaking & Steelmaking*, 1992. 19(3): p. 201-219.

[11] Chan, A.H. and R. Fruehan, The sulfur partition ratio and the sulfide capacity of Na_2O-SiO_2 slags at 1200 ℃. *Metallurgical and Materials Transactions B*, 1986. 17(3): p. 491-496.

[12] Wagner, C., S. Mellgren, and J.H. Westbrook, Thermodynamics of alloys. Vol. 4. 1952: Addison-Wesley Press.

[13] Suzuki, K., S. Ban-Ya, and M. Hino, Deoxidation equilibrium of Cr-Ni stainless steel with Si at the temperatures from 1 823 to 1 923 K. *ISIJ international*, 2002. 42(2): p. 146-149.

[14] Suzuki, K., S. Ban-Ya, and M. Hino, Deoxidation equilibrium of chromium stainless steel with Si at the temperatures from 1 823 to 1 923 K. *ISIJ international*, 2001. 41(8): p. 813-817.

[15] Deo, B. and R. Boom, Fundamentals of steelmaking metallurgy. 1993: Prentice Hall International.

[16] Miki, T. and M. Hino, Numerical Analysis on Si Deoxidation of Molten Fe, Ni, Fe-Ni, Fe-Cr, Fe-Cr-Ni, Ni-Cu and Ni-Co Alloys by Quadratic Formalism. *ISIJ international*, 2005. 45(12): p. 1848-1855.

[17] Roy, G., et al., Dephosphorization of ferromanganese using $BaCO_3$ based fluxes by submerged injection of powders: A preliminary kinetic study. *Metallurgical and Materials Transactions B*, 2001. 32(3): p. 558-561.

[18] Riboud, P. and R. Vasse, Désulfuration de l'acier en poche: synthèse des résultats théoriques et industriels. *CIT de la Revue de Metallurgie*, 1985. 82(11): p. 801-810.

[19] Persson, M., J. Zhang, and S. Seetharaman, A Thermodynamic Approach to a Density Model for Oxide Melts. *Steel Rresarch International*, 2007. 78(4): p. 290.

[20] Muhmood, L. and S. Seetharaman, Density Measurements of Low Silica CaO-SiO_2-Al2O_3 Slags. *Metallurgical and Materials Transactions B*. 2010. 41(4): p. 833-840.